Available online at www.sciencedirect.com
ScienceDirect
Trans. Nonferrous Met. Soc. China 26(2016) 2336−2346
Transactions of Nonferrous Metals Society of China
www.tnmsc.cn

Thermostability, mechanical and tribological behaviors of polyimide matrix composites interpenetrated with foamed copper

Li-peng WANG[1], Tao ZHANG[2], Lei ZHANG[1], Ji-si WU[1], Yan WANG[1], Ke-chao ZHOU[1]

1. State Key Laboratory of Powder Metallurgy, Central South University, Changsha 410083, China;
2. Shanghai Key Laboratory of Spacecraft Mechanism, Shanghai 201109, China

Received 23 September 2015; accepted 18 April 2016

Abstract: Polyimide matrix composites interpenetrated with foamed copper were prepared via pressure impregnation and vacuum immersion to focus on their thermostability, mechanical and tribological behaviors as sliding electrical contact materials. The results show that the interpenetrating phase composites (IPC) are very heat-resistant and exhibit higher hardness as well as bending strength, when compared with homologous polyimide matrix composites without foamed copper. Sliding electrical contact property of the materials is also remarkably improved, from the point of contact voltage drops. Moreover, it is believed that fatigue wear is the main mechanism involved, along with slight abrasive wear and oxidation wear. The better abrasive resistance of the IPC under different testing conditions was detected, which was mainly attributed to the successful hybrid of foamed copper and polyimide.
Key words: foamed copper; pressure impregnation; thermostability; mechanical properties; tribological behaviors

1 Introduction

With the rapid development of polymer materials, they have been widely applied in the field of tribology, such as polytetrafluoroethylene (PTFE), polyetheretherkrtone (PEEK), epoxy resin (EP), polyimide resin (PI) [1−3]. It is noticed for a long time that polymer materials show favorable mechanical properties, corrosion resistance and excellent chemical stability [4,5]. However, their electrical conductivity and thermal conductivity can be very poor, which limit their applications greatly because some products (such as pantograph slide plates, and motor brushes [6]) require specific conductivity. Once the friction heat accumulates at the interface which is hard to dissipate, the materials would deteriorate even fail with the rising temperature caused by the heat buildup [7]. Therefore, it is extremely urgent to improve the properties of polymers. Then, the compound of materials, especially the idea of interpenetrating phase composites (IPC), is an available way.

Nowadays, polymer materials are closely linked to IPC. IPC are multi-phase materials in which the constituent phases are interconnected three-dimensionally and topologically throughout the microstructure [8]. In this study, we introduce foamed copper skeletons into the PI to acquire an IPC. The foamed copper possesses numerous special properties, such as low density, specific mechanical performance, high specific surface area, and high conductivity [2]. Such continuous skeletons are able to play roles both in the improvement of polymer strength and enhancement of heat dissipation and electrical conductivity. Many researchers pay attention to the study of IPC. LI et al [9] studied on the copper foam-supported Sn thin film as a high-capacity anode for lithium-ion batteries and the film electrode showed good cycle performance. HONG and HERKING [10] researched open-cell aluminum foams filled with phase change materials as compact heat sinks, and found out that as the surface area density of foams raised, both the heating and cooling times of the testing sample increased. CREE and PUGH [11] discussed the dry wear and friction properties of A356/SiC foam IPC and obtained that the low friction coefficient and wear rate of the novel material provided the possible applications in light-weight fields.

At present, some relatively mature manufacturing processes of IPC have come into being. WANG et al [12] first prepared the porous preform via cold molding and sintering of the mixed dry PPS polymer powder and NaCl particles. Then, the porous preform was filled with

Corresponding author: Lei ZHANG; Tel: +86-731-88830464; E-mail: zhanglei@csu.edu.cn
DOI: 10.1016/S1003-6326(16)64355-8

lithium-base grease at 120 °C for 2 h under vacuum condition. Carbon/epoxy resin composites with an interpenetrating network structure were prepared with natural sponge and thermoset epoxy resin by injecting resin into the sponge, curing at 160 °C for 2 h [13]. WANG et al [14] introduced a new technology on preparation of IPC successfully. They infiltrated methyl methacrylate (MMA) adequately into the metal skeleton, and then exposed the materials with ^{60}Co γ-ray at 25 °C to induce in-situ bulk polymerization. Although lots of works on resin matrix composites interpenetrated with metal skeleton have been done, there are still many respects requiring further research.

In this study, the novel polyimide matrix composites interpenetrated with foamed copper were prepared by pressure impregnation and vacuum immersion. Here, polyimide resin, foamed copper, copper powder, MoS_2 and graphite were introduced as raw materials. MoS_2 and graphite are the most common but effective lubricants in the field of tribology material [15,16], while the copper powder is applied as an additive. The thermostability, mechanical properties, as well as friction and wear behaviors of composites were investigated in detail to better evaluate this novel material. Finally, this study is expected to provide a possibility of preparing advanced and practical sliding electrical contact materials.

2 Experimental

2.1 Materials

The foamed coppers, as indispensable components in the composites, were self-prepared by chemical plating on polyurethane (PU) sponge. Characteristics and mechanical parameters of foamed copper are given in Table 1. The apparent density of foamed copper is 0.22 g/cm^3, with 2.5 mm average aperture and 97.7% porosity.

Table 1 Characteristic parameters of foamed copper

Parameter	Foamed copper
Average aperture/mm	2.5
Porosity/%	97.7
Apparent density/(g·cm^{-3})	0.22
Compressive strength/MPa	0.37

Figure 1 shows the SEM images of raw material powders. It is noticed that the electrolytic copper powders have an average particle size of 15 μm with dendritic structures and PI powders show quite different particle sizes, while MoS_2 and colloidal graphite powders with similar irregular lamellar shapes are 7 μm

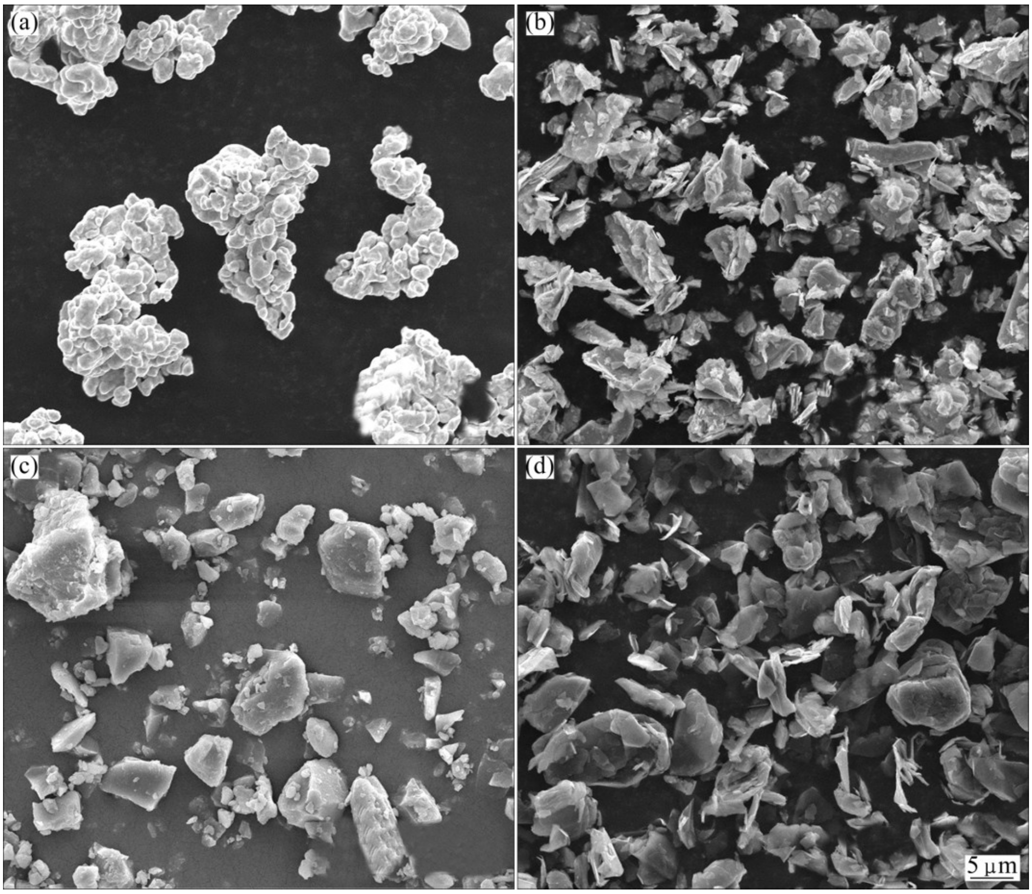

Fig. 1 SEM images of raw material powders: (a) Electrolytic copper; (b) MoS_2; (c) PI resin; (d) Colloidal graphite

in average particle size. The dimethylacetamide (DMAC) and ethanol solvents were also applied to preparing the slurry during experimental procedure.

2.2 Specimen preparation

The preparation of high porosity foamed copper skeletons with suitable stiffness is the first step in this study. After electroless plating copper on PU sponges, we removed the non-conductive sponge substrates by burning in a sintering furnace at 500 °C, deoxidized the foamed coppers at 900 °C for 2 h with H_2 protection, and finally cut them into 7 mm × 12 mm × 32 mm in size for further experiment, as shown in Fig. 2(a).

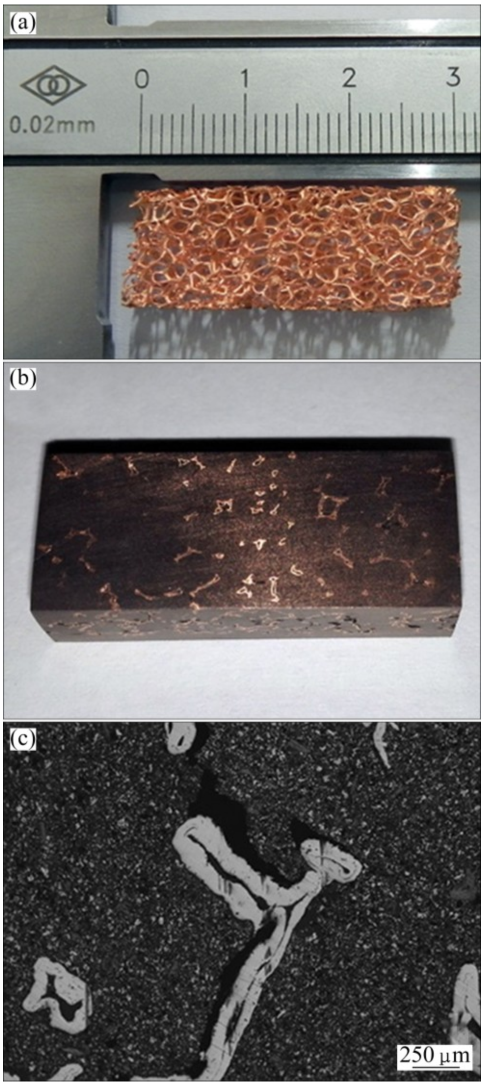

Fig. 2 Images of foamed copper and prepared sample: (a) Foamed copper; (b) Prepared sample; (c) Enlarged view of Fig. 2(b)

Next, the polyimide matrix composites interpenetrated with foamed copper as sliding electrical contact materials were fabricated by pressure impregnation, vacuum immersion and sintering as follows: DMAC and ethanol solvents were added into the mixed raw materials to form slurry with some certain liquidity; After the slurry was filled adequately into the foamed copper in a steel mould (12 mm × 32 mm) by fly press, the sample was heated in a vacuum drying oven at 170 °C for 2 h in order to remove the solvents totally. Finally, these green bodies were sintered at 230 °C for 2 h and then cooled down to room temperature naturally. The prepared sample is listed in Fig. 2. As can be seen from Fig. 2(c), the average coating thickness of foamed copper is around 100 μm.

In this work, two kinds of polyimide matrix composites interpenetrated with foamed copper and homologous PI-based polymer composites without copper foam (for comparison purpose) were studied. The compositional details are listed in Table 2. PI resin was incorporated into the composites at 45% (volume fraction) and this was in accordance with studies of LIU et al [17] and XIA at al [18], which revealed that the composites with 50% (volume fraction) resin content showed the best tribological behaviors. The three kinds of different samples were named as follows: PI/graphite (PI/G), PI/graphite/foamed copper (PI/G/FC), PI/MoS_2/ foamed copper (PI/MoS_2/FC), respectively.

Table 2 Compositions and ratios of samples (volume fraction, %)

Specimen	PI	MoS_2	Graphite	Copper
PI/G	45	0	34	21
PI/G/FC	45	0	34	21
PI/MoS_2/FC	45	34	0	21

2.3 Characterization

In order to better comprehensively evaluate the IPC, a series of tests were introduced. The DSC and TG tests were carried out by Netzsch STA 449C with 10 K/min in air; the macro Brinell hardness, the Vickers micro-hardness and the three-point bending testing with the samples of 6 mm × 10 mm × 30 mm in size were also measured. The average results were taken from three repeated tests.

The friction and wear properties of the composites were investigated by pin-on-disc form on the CSM tribometer. The size of specimen as pin was about 4 mm × 6 mm × 6 mm. The counterpart disc was made of copper alloy with Brinell hardness of HB 145 and Vickers micro-hardness of HV 171. The sliding friction and wear tests were carried out under a normal ambient condition ((50±5)% relative humidity, (20±5) °C) and the applied load was 2 N and 7 N, while the sliding velocity was 0.3 m/s and 1 m/s. An electric field (1 A constant current) was imposed between the specimen and disc to explore the contact resistance behaviors of sample by means of contact voltage drop. The wear rates of the specimens were calculated by the following equation:

$$w=\frac{\Delta m}{\rho FL} \tag{1}$$

In the equation, Δm is the mass loss of the specimen, ρ represents the density of the sample, F means the load applied to the composite, and L is the total sliding distance. In order to obtain insight into the wear mechanisms involved, the fracture microstructures as well as worn morphologies of samples, counterpart discs and wear debris were analyzed by optical microscope and field-emission scanning electron microscopy (FEI Company, Nova Nano SEM 230) equipped with EDS.

3 Results and discussion

3.1 Thermostability of composites

The thermostability of the composites was analyzed by DSC and TG test. Figure 3(a) shows that 230.3 °C is the curing temperature of PI resin, the first peak in the DSC curve. When it came to 350 °C, the PI resin started to react gradually and another exothermic peak appeared at 433.8 °C, along with the evident mass loss. After the whole test, it is found that 28.4% of its original mass is lost. The second exothermal event, which could represent the expulsion of the residual solvent enclosed in the polymer molecules, was overlapped on the beginning of the degradation process of the polymer. This process was possible due to the relaxation of the molecular chains during the glass transition phenomenon. A similar thermal event was observed on the DSC curve of PI coatings [1].

PI/G/FC and PI/MoS_2/FC have similar DSC curve in the early period and there are no peaks at 230 °C around, as shown in Figs. 3(b) and (c). It is believed that samples have been cured entirely. However, they display different exothermic peaks at 386, 352 and 382 °C, respectively, which are affected by other added components. The total mass losses are 2.5% and 9.54%, while the most mass loss of PI/G/FC is 4.76% at 380 °C. During the testing process, partial oxidation of copper powders and MoS_2 came up. Then, the former could make samples heavier and the latter lighter. Therefore, the results of TG curves are well reasonable. As can be seen from the above, the composites stay extremely stable before 300 °C in air.

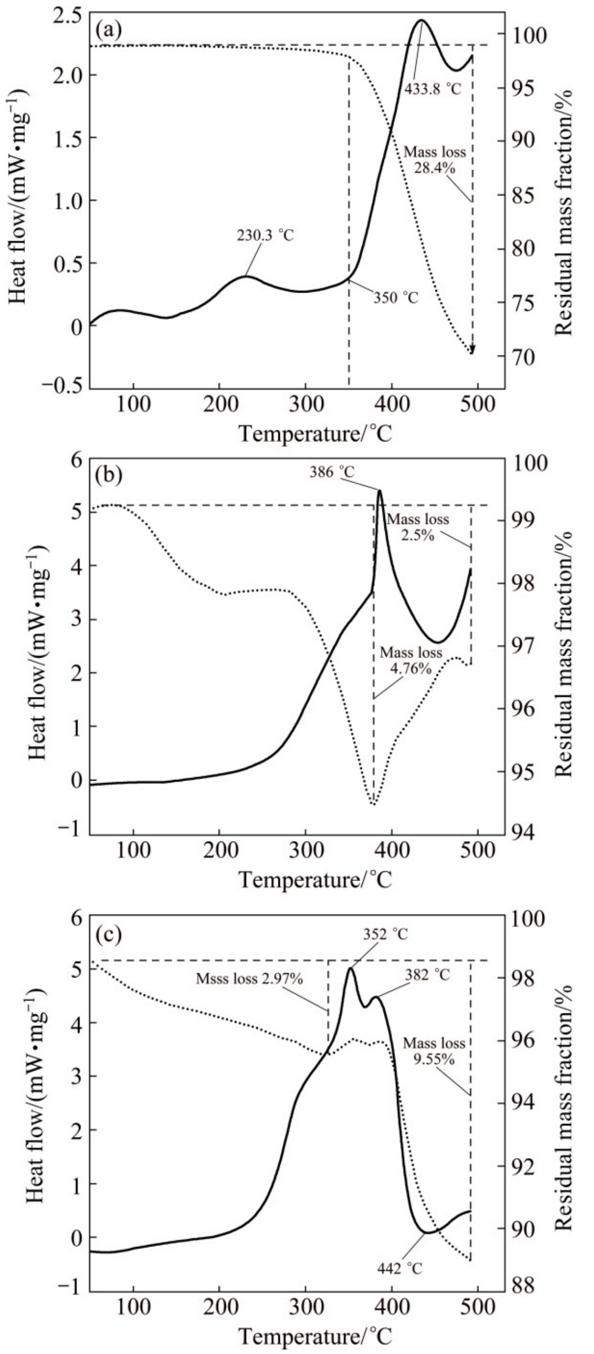

Fig. 3 DSC and TG data of samples in air: (a) PI; (b) PI/G/FC; (c) PI/MoS_2/FC

3.2 Mechanical properties

The density, Brinell hardness and bending strength of samples are presented in Table 3. It shows that the introduction of foamed copper contributes to compress the samples and increase the density of specimens. In addition, MoS_2 lubricant phase with high density results in the highest density of PI/MoS_2/FC. What's more,

Table 3 Mechanical properties of samples

Sample	Density/($g\cdot cm^{-3}$)	Brinell hardness	Bending Strength/MPa
PI/G	2.8	27	47.5
PI/G/FC	3.0	32	50.6
PI/MoS_2/FC	4.4	27	61.6

PI/G/FC has the highest Brinell hardness (HB 32), harder than PI/MoS_2/FC and PI/G (HB 27). This is rather consistent with the results of Vickers micro-hardness:

foamed coppers have the highest hardness (HV 50−80), MoS_2 has the lowest hardness (HV 20−30), and copper powder has the medium hardness (HV 27−32), respectively. Consequently, foamed copper reinforced the composites, while MoS_2 weakened them.

The addition of irregular MoS_2 powders into the PI matrix could not only improve the compactness of samples, but also cause better mechanically interlocked structure, which results in the increase of bending strength, as shown in Table 3. The foamed copper acting as the interconnected metal skeletons showed the same tendency. The bending strength of PI/MoS_2/FC is 61.6 MPa, increased by 21.7%, when compared to PI/G/FC (50.6 MPa); While the bending strength of PI/G/FC increased by 6.5%, compared to PI/G (47.5 MPa). HUANG et al [19] studied the friction and wear properties of Cu-based self-lubricating composites and observed the similar results.

After three-point bending testing, the fracture morphology of samples was examined by SEM, as shown in the Fig. 4. Every component exhibits homogeneous distribution and mechanically interlocked structure. Irregular MoS_2, dendritic structure of copper powder and foamed copper are easily identified. The foamed coppers were pulled out of the matrix and left hollow structure, as shown in Fig. 4(b). At the same time, raw constituents were extruded into the hollow structure, as shown in the Fig. 4(c). Figure 4(b) also shows the dimples and cellular network in the matrix, which are considered to be the residue appearance of dendritic structure copper powder. There is a gap between foamed copper and other component that can store lubricants and wear debris during the friction and wear testing, which contributes to abrasion performance, as stated in the study of QU et al [20]. What's more, MoS_2 flakes possess more irregular structure than colloidal graphite (as shown in Fig. 1), and PI resin is easier to infiltrate this rough surface, bringing about a higher bending strength. However, none of plastic deformation regions can be observed, which illustrates that only brittle rupture takes place.

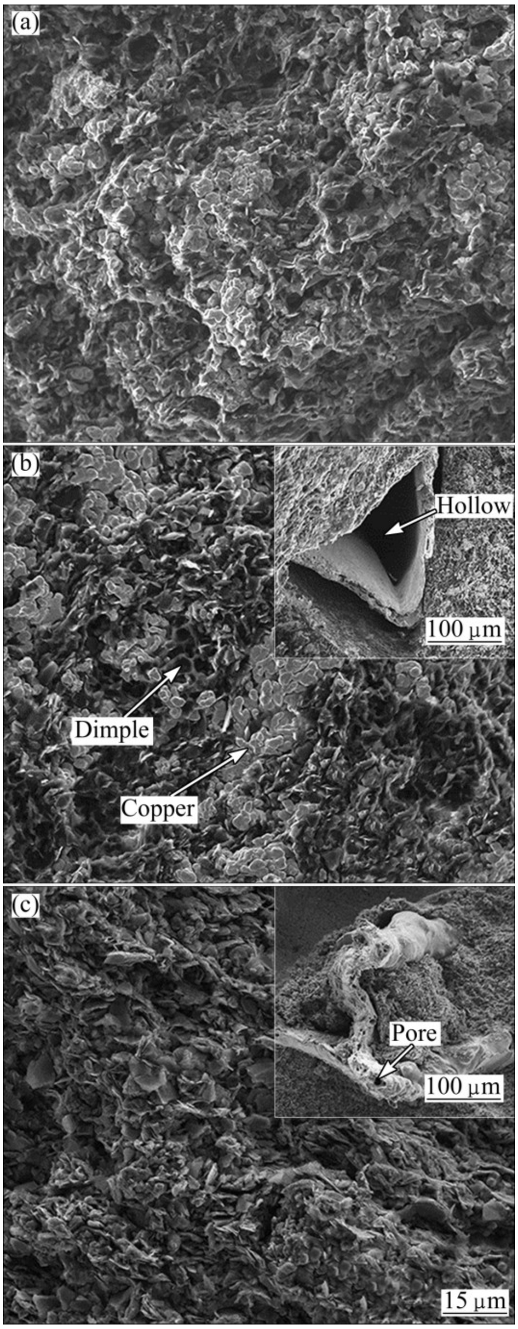

Fig. 4 SEM images of fracture morphology: (a) PI/G; (b) PI/G/FC; (c) PI/MoS_2/FC

3.3 Friction and wear properties

The friction coefficient curves of the samples as functions of sliding distances under different testing conditions are shown in Fig. 5. It can be seen that the friction coefficients of samples sliding against bronze disc display the similar value and trend under dry condition but different loads (2 N, 7 N), as shown in Figs. 5(a) and (b), respectively. The friction coefficients of PI/G and PI/G/FC are as low as 0.27, which are much less than PI/MoS_2/FC (0.4). Under electrical condition, the friction coefficients of samples show more distinction: PI/G/FC<PI/G<PI/MoS_2/FC, as shown in Fig. 5(c). In order to further study the effect of foamed coppers on the composites, the 2000 grit SiC abrasive papers were introduced as counterpart. Figure 5(d) shows that after a short run-in stage the friction coefficient remained quite stable and small (0.2, 0.23), which indicates that the integral transfer film quickly formed on the interface and roughness played a role in tribological behaviors of the composites. As for the high friction coefficient of PI/MoS_2/FC (both in dry condition and electrical circumstance), MoS_2 was not so efficient as a lubricant and might be decomposed into Mo oxide under air condition; when MoS_2 was squeezed out from the

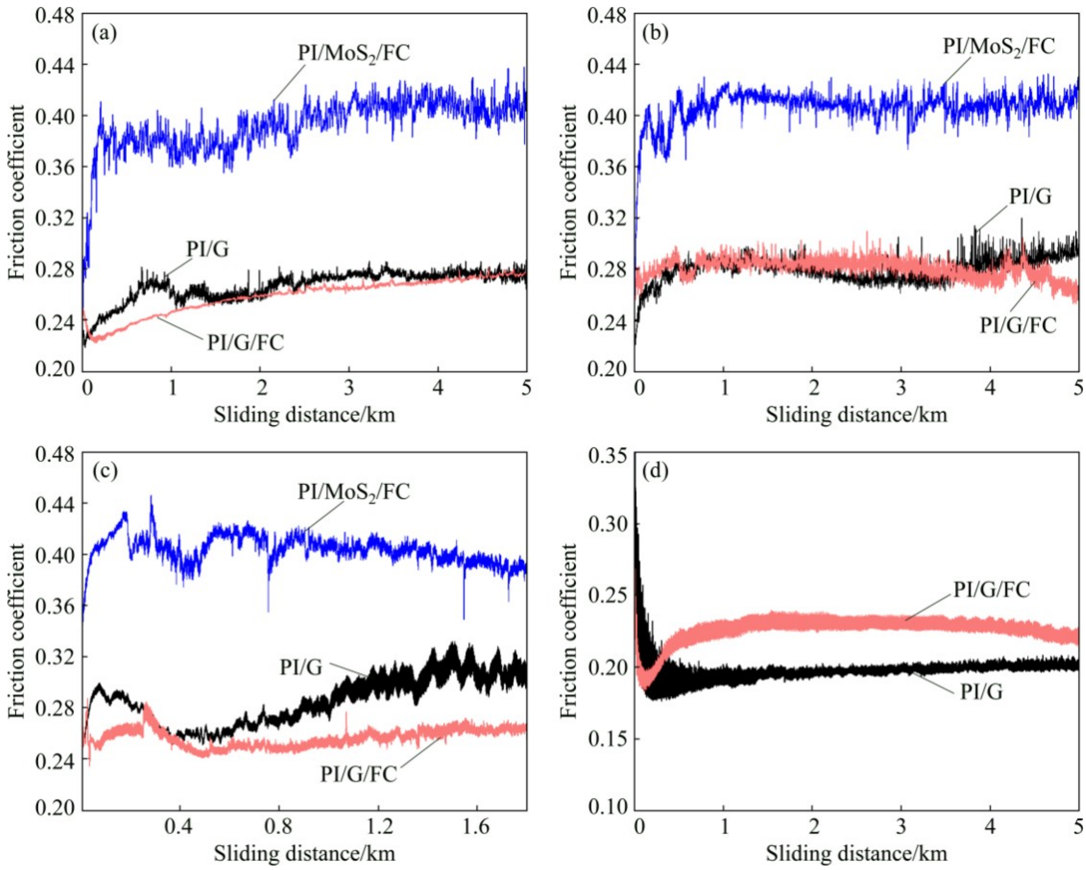

Fig. 5 Friction coefficient curves of samples sliding against bronze disc (a, b, c) and SiC abrasive papers (d) under dry condition (a, b, d) and electrical condition (c): (a) 7 N, 1 m/s; (b) 2 N, 1 m/s; (c) 7 N, 0.3 m/s; (d) 7 N, 0.3 m/s

subsurface of the matrix to the sliding surface, a part of it was scraped away by the tangential force. What's more, it is noted that colloidal graphite is easier to smear and adhere to counterpart disc, introducing a lubricant film between pin and disc. When the two active carbon atoms get close enough to each other, C—C bond is strongly bonded and hard to peel off [21], which results in low friction coefficient.

As can be seen in Fig. 6(a), the wear rates of samples under both dry and electrical conditions follow the rule obviously: PI/G/FC<PI/G<PI/MoS_2/FC, which is consistent with the law of average friction coefficients. However, the current affected samples inversely: it increased the wear rate of PI/MoS_2/FC and decreased PI/G's. According to the results of bending test, the foamed copper played a role in the reinforcement of the composites. In addition, the aperture between foamed copper and other components stored wear debris and lubricants effectively, which contributed to a better abrasive resistance. However, in the point of hardness property, MoS_2 is the softest phase and PI/MoS_2/FC has low Brinell hardness. What's more, the decomposition of MoS_2 in the process of friction and wear is also one reasonable explanation of its poor wear property, which has been confirmed by HU et al [22] and JI et al [23].

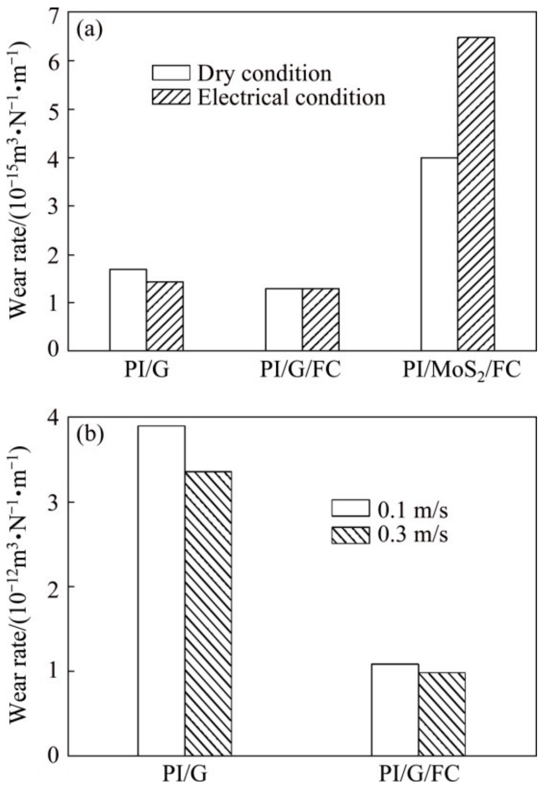

Fig. 6 Wear rates of samples under 7 N sliding against bronze disc (a) and SiC abrasive papers (b)

Therefore, PI/MoS_2/FC was easily scraped by hard phase and left more wear debris, resulting in highest wear rate (4.0×10^{-15} m^3/N·m). Besides, under the electrical condition testing, energy mostly diffused in the form of joule heat and finally instantaneous high temperature, appearing in contact spots, might destroy the PI polymer and MoS_2 structure, resulting in severer wear. As for PI/G, which lacked the load-sharing skeleton of foamed copper, it sustained more strain and was more likely to break down when exposed to the same load. Compared to Cu matrix composites containing graphite lubricant under the similar test condition, these wear rates were one or two magnitudes lower than the results of CAO et al [24] and LI et al [25].

Sometimes sliding electrical contact materials need to be served under rough interface, so the sliding against sandpaper testing is necessary. Though the order of magnitude of wear rate rises to 10^{-12} m^3/(N·m), the PI/G and PI/G/FC present more significant difference in abrasive resistance. In addition, it can be found that with the increase of sliding speed, the wear rates show a little reduction, as shown in Fig. 6(b). When the samples slid against sandpapers, contact surface was scraped by SiC particles and wear debris was left on the interface or out of wear track. As the sliding speed increased, the transfer film formed earlier and a better contact condition took place, resulting in lower wear rate. All in all, these IPC demonstrated admirable anti-wear performance under these study criteria.

3.4 Analysis of worn surfaces and wear debris

Figure 7 exhibits the worn morphologies of samples under 7 N. The worn surfaces of the composites can be divided into two areas: metallic skeleton area and polymeric area. There are no big differences in worn morphology between dry condition and electrical circumstance. The wear scars on the metallic skeleton mainly present smooth, but part of them show the rough subsurface after peeling of surface layer, which is affected by cyclic stress and crack growth through the weak regions. Ploughed marks and fine wear debris can be found on the contact surface along the sliding direction, especially as shown in Figs. 7(a) and (f). This rough morphology and wear debris exactly agree with the rule of wear rate: the introduction of current increased the wear rate of PI/MoS_2/FC and decreased that of PI/G, compared to dry condition. It can be noted that the copper powders were lengthened and squeezed as plastic flow during sliding friction, which was restrained by the foamed copper skeleton. Figure 7(c) shows the pores on the friction surface, remaining the original morphology of foamed copper. The worn surfaces of PI/G/FC sample under both dry and electrical conditions show flatter interface, indicating that the transfer film well formed, so the friction coefficient and wear rate are low.

In order to better figure out the wear mechanism, the worn morphology of counterpart bronze disc was analyzed by optical microscope. Some graphite, MoS_2 and polymeric wear debris had adhered to the surfaces of counterpart disc, which can be distinguished by the changes of surface morphology. Foamed copper, the hardest component of the composites, as well as wear debris trapped between the two contact surfaces scraped and micro-cut the bronze disc constantly during sliding friction, leaving plenty of furrows on the disc surface

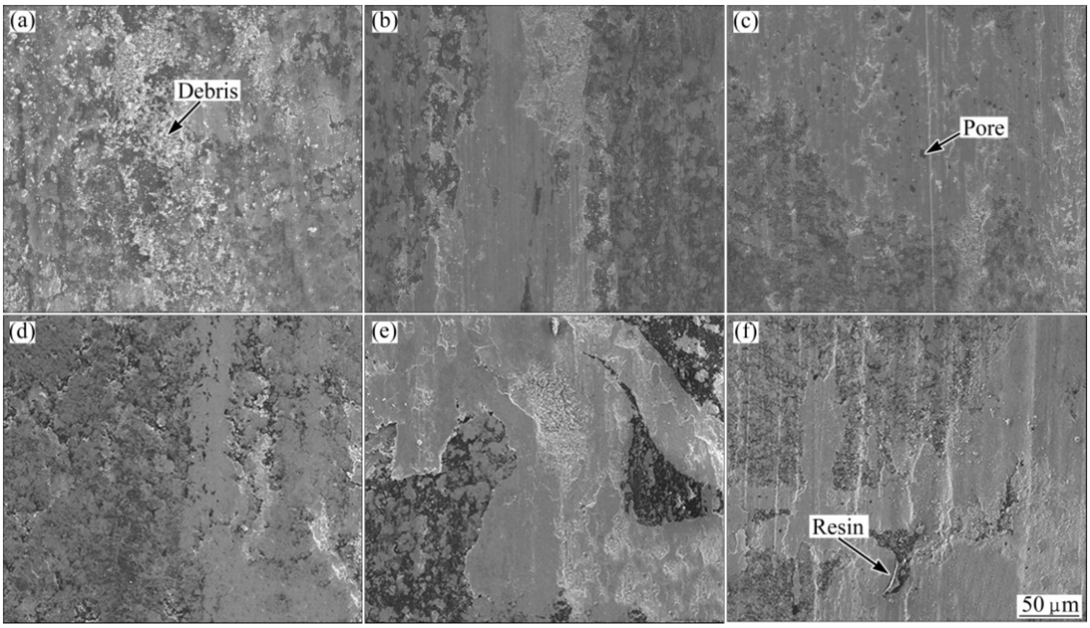

Fig. 7 SEM images of worn surfaces under dry condition (a, b, c) and electrical condition (d, e, f): (a, d) PI/G; (b, e) PI/G/FC; (c, f) PI/MoS_2/FC

along the sliding direction, as shown in the Fig. 8. What's more, some wear debris stuck to the disc by cohesive force and adsorption capacity, accompanying with plastic flow. As can be seen in Figs. 8(b) and (e), more lubricant films developed on the surface of the bronze disc running against PI/G/FC than the disc matching PI/MoS_2/FC, so PI/G/FC performed better than PI/MoS_2/FC in both friction coefficient and wear rate respects. Furthermore, compared with dry condition testing, the worn morphology of samples under electrical circumstance was smoother, which may be concerned with the contrast of friction heat.

Figure 9 displays the wear debris after friction and wear test. Three kinds of shapes are clearly identified: large sheet, small flake and tiny fine. Large sheets are mainly found under the dry sliding condition. During sliding friction, cracks first generated in defective locations under the action of cyclic stress, and expanded along the weakly combined areas, finally surface layer was peeled off from the matrix as large sheet. Afterwards, some sheets between two contact interfaces were impacted and ground by positive pressure and tangential

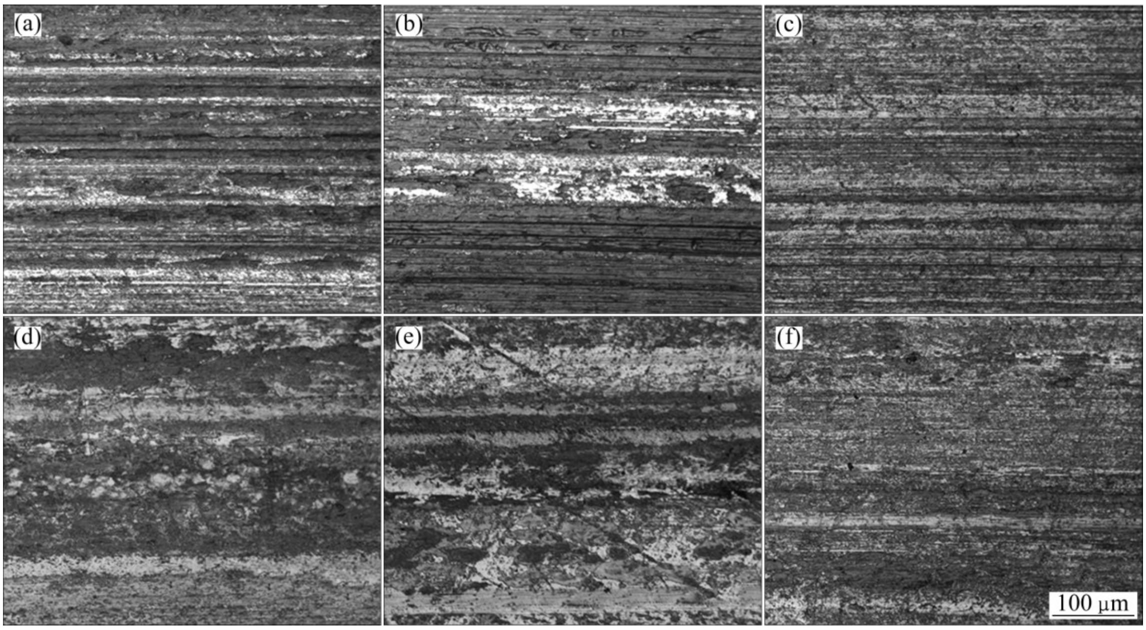

Fig. 8 Optical images of worn surfaces of copper disc sliding against PI/G (a, d), PI/G/FC (b, e) and PI/MoS_2/FC (c, f) under dry condition (a, b, c) and electrical condition (d, e, f)

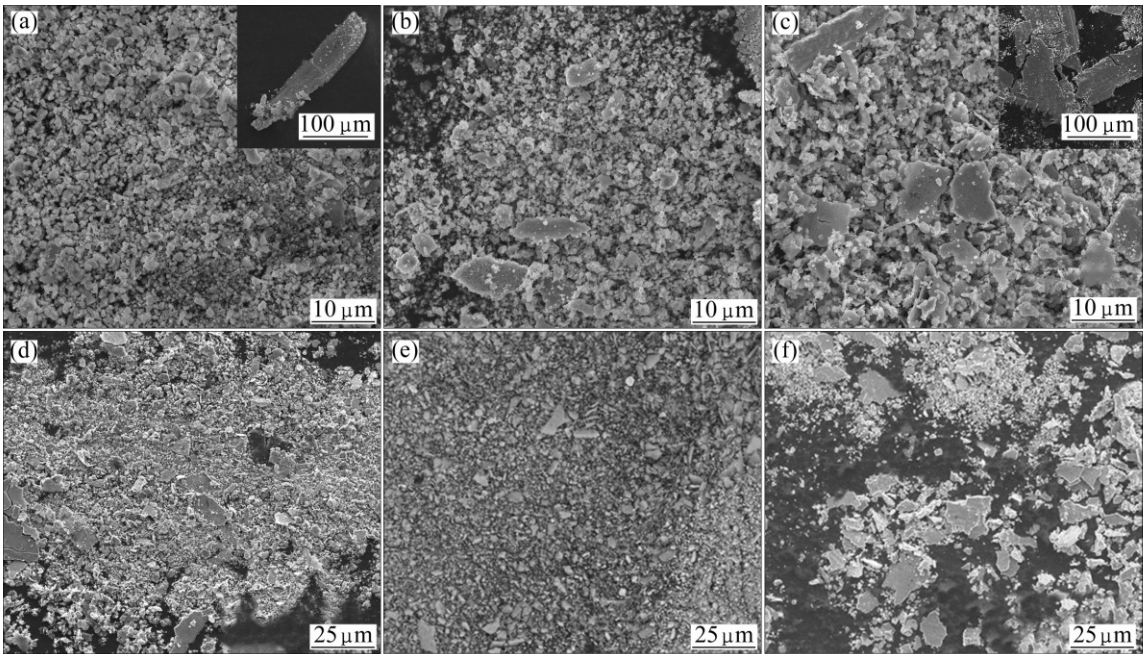

Fig. 9 SEM images of wear debris under dry condition (a, b, c) and electrical condition (d, e, f): (a, d) PI/G; (b, e) PI/G/FC; (c, f) PI/MoS_2/FC

force, resulting in small flake or tiny fine, while others were just taken away from sliding track by tangential force, keeping the large strip shape. EDS analysis of PI/MoS_2/FC demonstrated that the wear debris came from the sample and counterpart disc.

As can be seen from Fig. 10, wear debris consists of Cu, O, C, Mo, S, Zn elements and the mole ratio of Mo and S is nearly 1:2, which reveals that MoS_2 exists at the friction interface in the way of transfer film. C element is considered as the decomposition product of PI resin and Zn element is from the bronze counterpart disc. O element shows that oxidation of the worn surface is certain in the friction and wear process. According to GAO et al [26], copper alloys have a strong tendency to be oxidized and oxidation can be the main wear mechanism. However, in our study, it can be concluded that fatigue wear was the main mechanism involved, along with abrasive wear and oxidation.

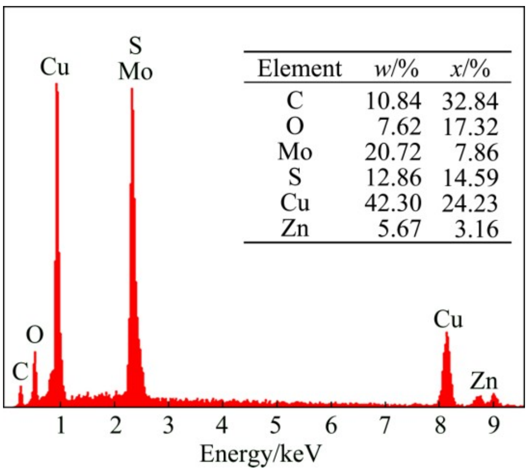

Fig. 10 EDS analysis of wear debris: PI/MoS_2/FC sliding against bronze disc under dry condition

3.5 Contact voltage drop

When the samples are applied under the current condition, the contact resistance is one of important performance indexes. In this work, the contact resistance is researched by contact voltage drop. As can be seen from Fig. 11, PI/G shows quite high average voltage drop (1.7 V), while the other three have similar values range from 0.2 to 0.4 V, decreased by 76.5%−88.2%. What is more, the curves are relatively stable, compared to PI/G sample. QIAN et al [27] tested the contact voltage drop of Cu/graphite/WS_2 composites with high copper content against CuAg5 alloy ring and got the similar result of 0.25−0.45 V. Modern scientific researches hold that the contact resistance consists of bulk resistance, contraction resistance and velamen resistance [6], but it mostly depends on the circumstance of contact interface.

Basically, contact interface contains transfer films and wear debris. To some extent, the contact resistance is inversely related to the contact area. There is no doubt that foamed copper embedded in polymer matrix plays a role in conductive property of the composites. The foamed copper can not only decrease the bulk resistance by offering fast transport channel of charge carriers, but also produce more direct contact spots in contact interface, which results in low voltage drop. The study of CHEN et al [28] revealed that electrons moved quickly through the interconnected 3D network, resulting in high electrical conductivity. Furthermore, nearly no changes of electrical conductivity of the graphene networks happened after having been infiltrated with polymer materials. As the IPC, the foamed copper is an independent continuous phase, so we can reasonably consider that it is in parallel with other components under electrical wear test. Therefore, voltage drops of the latter two samples exhibit no much difference.

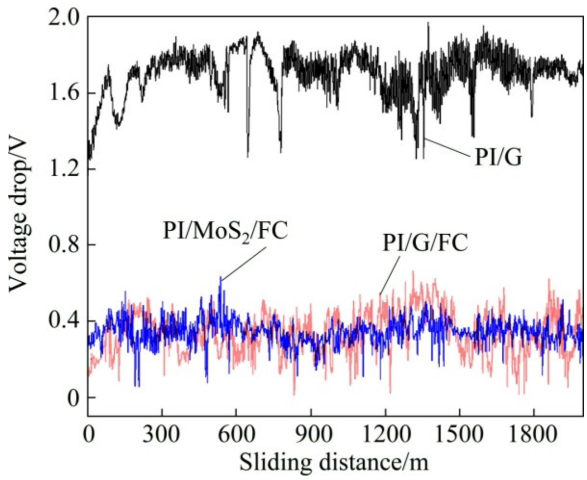

Fig. 11 Contact voltage drop curves of samples under 7 N and 0.3 m/s

4 Conclusions

1) The composites stay extremely stable before 300 °C in air, which provides the potential of high temperature application.

2) The IPC samples showed a slight improvement in hardness and bending strength due to the load-sharing of the interconnected metal skeleton, compared with those without foamed copper.

3) Under all the different testing conditions (electrical, speed and load), the PI/G/FC samples always exhibit better abrasive resistance than PI/G, which can mainly be attributed to the enhancement effect of foamed copper.

4) The large sheets, small flakes, tiny fines as well as furrows on the worn surfaces of specimens and counterpart discs reveal that fatigue wear is the main mechanism involved, along with the abrasive wear and

oxidation simultaneously.

5) The contact voltage drops of IPC samples (from 0.2 to 0.4 V) decrease by 76.5%−88.2%, compared to specimen without foamed copper (1.7 V). It can be concluded that the contact property under current condition is remarkably improved.

References

[1] DEMIAN C, LIAO H L, LACHAT R, COSTIL S. Investigation of surface properties and mechanical and tribological behaviors of polyimide based composite coatings [J]. Surface and Coatings Technology, 2013, 235: 603−610.

[2] BURRIS D L, SAWYER W G. Hierarchically constructed metal foam/polymer composite for high thermal conductivity [J]. Wear, 2008, 264: 374−380.

[3] JI Ke-ju, XU Yin-song, ZHANG Jun, CHEN Jia, DAI Zhen-dong. Foamed-metal-reinforced composites: Tribological behavior of foamed copper filled with epoxy-matrix polymer [J]. Materials and Design, 2014, 61: 109−116.

[4] WANG X Y, MA J X, LI C G, WANG H X. Thermosetting polyimide resin matrix composites with interpenetrating polymer networks for precision foil resistor chips based on special mechanical performance requirements [J]. Applied Surface Science, 2014, 299: 73−80.

[5] ZHAO Gai, HUSSAINOVA I, ANTONOV M, WANG Qi-hua, WANG Ting-mei. Friction and wear of fiber reinforced polyimide composites [J]. Wear, 2013, 301: 122−129.

[6] BRAUNOVIC M, KONCHITS V V, MYSHKIN N K. Electrical Contacts: Fundamentals, applications and technology [M]. Florida: CRC Press, 2006: 117−121.

[7] WIELEBA W. The role of internal friction in the process of energy dissipation during PTFE composite sliding against steel [J]. Wear, 2005, 258: 870−876.

[8] JHAVER R, TIPPUR H. Processing, compression response and finite element modeling of syntactic foam based interpenetrating phase composite (IPC) [J]. Materials Science and Engineering A, 2009, 499: 507−517.

[9] LI Qing-yu, HU Si-jiang, WANG Hong-qiang, WANG Fang-ping, ZHONG Xin-xian, WANG Xin-yu. Study of copper foam-supported Sn thin film as a high-capacity anode for lithium-ion batteries [J]. Electrochimica Acta, 2009, 54: 5884−5888.

[10] HONG S T, HERKING D R. Open-cell aluminum foams filled with phase change materials as compact heat sinks [J]. Scripta Materialia, 2006, 55: 887−890.

[11] CREE D, PUGH M. Dry wear and friction properties of an A356/SiC foam interpenetrating phase composite [J]. Wear, 2011, 272: 88−96.

[12] WANG Huai-yuan, LIU Du-juan, YAN Lei, LI Mei-ling, WANG Chao, ZHU Yan-ji. A computed model for tribological properties of porous self-lubricating PPS composites: Numerical analysis and experimental verification [J]. Wear, 2014, 320: 94−102.

[13] WANG Tian-chi, XIONG Dang-sheng, ZHOU Tian-le. Preparation and wear behavior of carbon/epoxy resin composites with an interpenetrating network structure derived from natural sponge [J]. Carbon, 2010, 48: 2435−2441.

[14] WANG Mo-zhen, GENG Hong-wei, GE Xue-wu, LI Jian-rong, KOU Dong-peng. Polymer/metal interpenetrating phase composites prepared via γ-ray initiated in-situ emulsion polymerization [J]. Polymer Composites, 2009, 30(9): 1258−1263.

[15] SENOUCI A, FRENE J, ZAIDI H. Wear mechanism in graphite−copper electrical sliding contact [J]. Wear, 1999, 22(98): 949−953.

[16] KATO H, TAKAMA M, IWAI Y, WASHIDA K, SASAKI Y. Wear and mechanical properties of sintered copper−tin composites containing graphite or molybdenum disulfide [J]. Wear, 2003, 255: 573−578.

[17] LIU Pei, LU Ren-guo, HUANG Ting, WANG Hong-yan, LI Tong-sheng. A study on the mechanical and tribological properties of carbon fabric/PTFE composites [J]. Journal of Macromolecular Science, Part B: Physics, 2012, 51: 786−797.

[18] XIA Jin-tong, HU Zhong-liang, CHEN Zhen-hua, DING Guo-yun. Preparation of carbon brushes with thermosetting resin binder [J]. Transactions of Nonferrous Metals Society of China, 2007, 17: 1379−1384.

[19] HUANG Shi-yin, FENG Yi, DING Ke-wang, QIAN Gang, LIU Hong-juan, WANG Yang. Friction and wear properties of Cu-based self-lubricating composites in air and vacuum conditions [J]. Acta Metallurgica Sinica, 2012, 25(5): 391−400.

[20] QU J, BLAU P J, KLETT J, JOLLY B. Sliding friction and wear characteristics of novel graphitic foam materials [J]. Tribology Letters, 2004, 17(4): 879−885.

[21] XIAO Jin-kun, ZHANG Lei, ZHOU Ke-chao, LI Jian-guo, XIE Xin-lin, LI Zhi-you. Anisotropic friction behaviour of highly oriented pyrolytic graphite [J]. Carbon, 2013, 65: 53−62.

[22] HU Zhong-liang, CHEN Zhen-hua, XIA Jin-tong, DING Guo-yun. Wear property of high-resistivity carbon brushes made with and without MoS_2 in variable humidity [J]. Transactions of Nonferrous Metals Society of China, 2008, 18: 340−345.

[23] JI Ke-ju, SHAN Wei-gen, XIA Yan-qiu, DAI Zhen-dong. The tribological behaviors of self-lubricating composites as filler in copper foam [J]. Tribology Transactions, 2012, 55: 20−31.

[24] CAO Hui-quan, QIAN Zhi-yuan, ZHANG Lei, XIAO Jin-kun, ZHOU Ke-chao. Tribological behavior of Cu matrix composites containing graphite and tungsten disulfide [J]. Tribology Transactions, 2014, 57: 1037−1043.

[25] LI Jing-fu, ZHANG lei, XIAO Jin-kun, ZHOU Ke-chao. Sliding wear behavior of copper-based composites reinforced with graphene nanosheets and graphite [J]. Transactions of Nonferrous Metals Society of China, 2015, 25(10): 3354−3362.

[26] CAO Yuan, JIE Jin-chuan, ZHANG Peng-chao, ZHANG Jian, WANG Tong-min, LI Ting-ju. Wear behavior of high strength and high conductivity Cu alloys under dry sliding [J]. Transactions of Nonferrous Metals Society of China, 2015, 25(7): 2293−2300.

[27] QIAN Gang, FENG Yi, CHEN Yang-ming, MO Fei, WANG Yu-qing, LIU Wen-hong. Effect of WS_2 addition on electrical sliding wear behaviors of Cu−graphite−WS_2 composites [J]. Transactions of Nonferrous Metals Society of China, 2015, 25(6): 1986−1994.

[28] CHEN Zong-ping, REN Wen-cai, GAO Li-bo, LIU Bi-lu, PEI Song-fei, CHENG Hui-ming. Three-dimensional flexible and conductive graphene networks grown by chemical vapour deposition [J]. Nature Materials, 2011, 10: 424−427.

泡沫铜/聚酰亚胺互穿型复合材料的制备及其热稳定性和力学与摩擦性能

王立鹏[1]，张 涛[2]，张 雷[1]，吴集思[1]，王 艳[1]，周科朝[1]

1. 中南大学 粉末冶金国家重点实验室，长沙 410083；
2. 上海宇航系统工程研究所，上海 201109

摘 要：采用压力浸渍和真空渗透的工艺制备了泡沫铜/聚酰亚胺互穿型复合材料，并重点研究了其作为滑动电接触材料的热稳定性，力学性能与摩擦磨损等方面性能。实验结果表明：该互穿型复合材料具备良好的耐热性，同时与不含泡沫铜的聚酰亚胺树脂基复合材料相比，其布氏硬度及抗弯强度等力学性能有一定的提高，滑动电接触性能从电压降的角度来说则有显著的改善。其次，研究发现该材料的磨损机制主要为疲劳磨损，同时伴随着轻微的磨粒磨损和氧化磨损。该材料在不同实验条件下都显示出较好的耐磨性，这表明泡沫铜与聚酰亚胺复合后的互穿型结构起了关键作用。

关键词：泡沫铜；加压浸渍；热稳定性；力学性能；摩擦性能

(Edited by Yun-bin HE)